Int. J. Solids Structures Vol. 30, No. 14, pp. 1919–1937, 1993
Printed in Great Britain

0020–7683/93 $6.00+ .00

INTERACTIONS AMONG CRACKS AND RIGID LINES NEAR A FREE SURFACE

KAI XIONG HU and ABHIJIT CHANDRA
Department of Aerospace and Mechanical Engineering, The University of Arizona, Aero Building 16, Tucson, AZ 85721, U.S.A.

(*Received* 6 *February* 1992; *in revised form* 8 *January* 1993)

Abstract—Cracks and rigid-line inclusions, or anticracks, are commonly observed in many engineering materials, such as intermetallics and ceramic composites. Interactions among these cracks and rigid lines can significantly affect the strength of these materials. Strength degradation due to finishing operations, such as grinding, also depend to a large extent on these interactions near a free surface and their associated surface and subsurface damage evolutions. Accordingly, modeling of interactions among general systems of cracks and rigid lines in the vicinity of a free surface, subject to general loading conditions, is the main thrust of this paper. An integral equation approach based on the fundamental solutions due to point loads and point dislocations in an elastic half plane is utilized for this purpose. The integral equations are reduced to a system of linear equations consisting of the distributions of Burger's dislocation vectors and forces on the cracks and the anticracks, respectively. The proposed solution procedure also allows direct determination of the rigid-body rotations for the rigid lines. The results obtained from the present analysis are first verified against existing results for a single crack or rigid line near a free surface. The amplification and shielding effects on stress intensity factors due to interactions among various distributions of cracks and rigid lines are then investigated. Such interactions near a free surface play crucial roles in surface and subsurface damage evolutions during high-speed machining of ceramic materials.

1. INTRODUCTION

Most common engineering materials contain defects in the form of cracks, voids or rigid inclusions that can significantly affect their load-carrying capacities. In recent years, various ceramic compounds and intermetallics, by virtue of possessing ordered superlatice structures and high activation energies for diffusion, have been found to be ideally suited for high-temperature strength and modulus retention. However, these ceramic compounds and intermetallics are generally very brittle at room temperature. In order to enhance the ductility at room temperature and to lower the brittle–ductile transition temperatures, various researchers have attempted to change the crystal structures using alloys. The alloying agents, however, introduce second-phase particles in the matrix. The networks of microdefects (voids or inclusions) introduced through alloying can significantly affect the final strength and characteristics of the products. In many material processing and structural applications, the interactions among these microdefects (voids or inclusions) have been observed to be one of the important factors in determining the macro-failure modes [e.g. Kachanov (1985), Horii and Nemat-Nasser (1986), Baeslack *et al.* (1988), Haritos *et al.* (1988) and Jha *et al.* (1988)].

For ceramics and intermetallics, this network of microdefects and their associated brittle fracture modes provide crucial avenues for material removal processes. As shown by Hu and Chandra (1992a), the apparent moduli of an ultrahard ceramic material may be reduced to less than 40% of the original values by inducing predetermined distributions of microcracks. This ability to control apparent moduli has very important ramifications for various material removal processes, such as grinding, drilling, etc. For grinding of ceramics, the surface and subsurface damage evolution is also significantly influenced by the interactions among cracks generated due to grinding and the pre-existing microcracks (Hu and Chandra, 1993a). For such material removal processes, the interactions occur near a free surface, and it has been observed that the free surface greatly modifies the nature of these interactions.

Two kinds of microdefects are typically observed in a material. The first one is a microvoid, which can also be idealized as a microcrack. A crack is essentially a cut that

transmits no traction across it, but allows a displacement discontinuity. The other type of microdefect is a rigid inclusion. A rigid lamella may be modeled as the opposite of a crack, i.e. it transmits tractions but prevents displacement discontinuity. Moreover, rigid lamella can undergo only rigid-body motions and no deformations. Dundurs and Markenscoff (1989) also refer to these rigid lines as anticracks. In addition to representing harder inclusions, rigid lines may also be used to model the fibers or whiskers in a metal-matrix or ceramic-matrix composite material. Many advanced materials for cutting tools belong to this category, and interactions among rigid lines and microcracks near a free surface must be considered in order to model damage evolutions in such applications. Many structural composite components may also require surface finishing, and interactions among rigid lines and cracks near a free surface need to be understood thoroughly in order to comprehend the extent of damage induced by such operations. Accordingly, the investigation of interactions among general systems of cracks and rigid lines near a free surface is the main thrust of this paper. An integral equation approach based on the fundamental fields due to point loads and point dislocations near a free surface is utilized for this purpose. A Gauss-Chebychev quadrature is used to reduce the integral equations to a linear system of equations consisting of the distribution of forces and Burger's dislocation vectors on the rigid lines and cracks, respectively. The proposed solution procedure also allows direct determination of the rigid-body rotations for the rigid lines.

This paper starts with a review of the literature relevant to problems involving cracks and rigid lines, followed by a presentation of fundamental solutions due to point loads and point dislocations near a free surface. An integral equation formulation for general systems of cracks and rigid lines near a free surface is developed next. The numerical results obtained by the proposed technique are first verified against existing solutions for a single crack or a rigid line near a free surface. General systems of cracks and rigid lines in the vicinity of a free surface subject to general loading conditions are considered next, and the proposed technique is used to investigate the amplification and shielding effects in such systems. Implications of such interactions, or damage evolutions, during ceramic grinding are also discussed. It is also interesting to note that, for a given configuration, the interactions between two cracks and between a crack and a rigid line bound the range of all possible interaction effects.

2. BACKGROUND

The problems involving rigid lines, or anticracks, have also been widely investigated in the context of elasticity. An extensive review of elastic problems involving inclusions is given by Mura (1987, 1988). Initial work on rigid-line inclusions can be traced back to Muskhelishvili (1953) and Eshelby (1957, 1959). Since then, problems involving rigid-line inclusions have been investigated by several researchers [e.g. Atkinson (1973), Brussat and Westmann (1975), and Hasebe *et al.* (1984)] for isotropic elastic bodies. Chou and Wang (1983) and Wang *et al.* (1985, 1986) considered a rigid-line inclusion in an isotropic planar elastic body and derived analytical expressions for the stress field due to uniform remote loading. The same problem has also been considered by Ballarini (1987) using an integral transform method. Sendeckyj (1970) and Selvadurai (1980) investigated elastic-line inclusions. Atkinson (1973) also considered elastic-line inclusions, and a solution for a half plane containing an anticrack perpendicular to the free surface is given. He obtained an asymptotic solution for the stress fields under the assumption that the inclusion is much harder than the matrix. Erdogan and Gupta (1972) studied the more general problem of bonded materials containing a flat inclusion that may be rigid or elastic with negligible bending rigidity. They formulated the problem as a system of singular integral equations that is solved by expanding the solutions in Chebychev polynomials. Dundurs and Markenscoff (1989) provide a direct Green's function formulation for rigid lines. Such a formulation is very suitable for solution by currently available numerical methods. They also provide pertinent fields for concentrated forces, dislocations, and couples applied on the line of the anticrack. Li and Ting (1989) investigated line inclusions embedded in an anisotropic infinite elastic medium subject to uniform remote loading. Stroh's (1958, 1962) formalism

is used to obtain the displacement and stress fields. They consider both rigid and elastic inclusions. A pair of singular Fredholm integral equations of the second kind is derived for the difference in the stress on both surfaces of an elastic and anisotropic inclusion. If the relative rigidity of the matrix is small compared to that of the inclusion, Li and Ting (1989) showed that the governing equations can be decoupled. For such rigid-line cases, they also obtain asymptotic solutions for the traction and the rotation of the rigid line.

Most of the existing analyses including rigid lines, however, consider a single rigid-line inclusion. On the other hand, problems involving interacting cracks have been studied more extensively. Goldstein and Salganik (1974) studied brittle fracture of solids with arbitrary cracks. Utilizing the superposition technique and the ideas of self-consistency applied to the average tractions on individual cracks, Kachanov (1985, 1987) obtained approximate analytical solutions for the stress intensity factor due to interacting elastic cracks. Melin (1983) and Broberg (1987) investigated the directional stability of cracks using linear elastic fracture mechanics and observed that the interactions among cracks significantly influence the directional stability and crack branching characteristics. Hori and Nemat-Nasser (1987) also used the method of Muskhelishvili to obtain a two-dimensional elasticity solution for interacting microcracks near the tip of a macrocrack. Using a dislocation approach, various researchers have also reduced the problem of a linear elastic solid with interacting cracks to a system of integral equations [e.g. Chatterjee (1975), Erdogan and Gupta (1975), Lo (1978, Cotterell and Rice (1980), Melin (1986), Chudnovsky *et al.* (1987a,b), and Müller (1989)].

The problem of a half plane containing a crack has been studied by several researchers [e.g. Ioakimidis and Theocaris (1979), Keer *et al.* (1982), Keer and Bryant (1983), Chen (1984), Nowell and Hills (1987), and Li and Hills (1990)]. Recently, Hu and Chandra (1993a) used an integral equation approach to investigate the interactions among cracks near a free surface and their implications on surface degradation during grinding of ceramics. A force-type integral equation, where the kernels contain only weak logarithmic singularities and the unknowns are Burger's vectors on the crack faces, was developed by Cheung and Chen (1987) for a full plane problem containing cracks. Zang and Gudmundson (1989, 1991) extended the approach to analyse half plane and anisotropic problems.

As discussed before, the problems involving interactions among cracks and anticracks are of crucial significance for understanding various physical phenomena ranging from failure of alloys containing second-phase particles to chip formation mechanics in ceramic grinding processes. In spite of thsese practical implications, problems involving interactions of cracks and anticracks have received relatively little attention so far. Brussat and Westmann (1975) investigated the interactions among collinear rigid-line inclusions subject to uniform remote loading. For this special case, they establish a direct correspondence between the Westergaard stress function for elastic crack problems and a stress function for rigid-line inclusion problems. A correspondence is also shown to exist between crack opening displacements and axial forces on the rigid inclusions.

3. FUNDAMENTAL FIELDS DUE TO POINT LOADS AND POINT DISLOCATIONS

An integral equation approach is pursued here to investigate the interactions among general systems of cracks and rigid lines near a free surface subject to general loading conditions. Cracks and rigid lines can be modeled as continuous spatial distributions of dislocations and tractions. Accordingly, the corresponding fundamental solutions due to a point load and a point dislocation are discussed in this section. Two-dimensional problems are considered here.

For a two-dimensional elastic half plane ($x \geqslant 0$) subjected to a concentrated force with components p_x and p_y at the location $(\xi, 0)$, the solutions due to Dundurs and Hetenyi (1961) and Hetenyi and Dundurs (1962) at a point (x, y) may be written as

$$2Gu_{x,x} = \frac{1}{2\pi(\kappa+1)}[p_x H_1(x, y; \xi) + p_y H_2(x, y; \xi)], \tag{1a}$$

$$2Gu_{x,y} = \frac{1}{2\pi(\kappa+1)}[p_x H_3(x,y;\xi)+p_y H_4(x,y;\xi)], \tag{1b}$$

$$2Gu_{y,x} = \frac{1}{2\pi(\kappa+1)}[p_x H_5(x,y;\xi)+p_y H_6(x,y;\xi)], \tag{1c}$$

$$2Gu_{y,y} = \frac{1}{2\pi(\kappa+1)}[p_x H_7(x,y;\xi)+p_y H_8(x,y;\xi)], \tag{1d}$$

$$\sigma_{xx} = \frac{1}{2\pi(\kappa+1)}[p_x H_9(x,y;\xi)+p_y H_{10}(x,y;\xi)], \tag{1e}$$

$$\sigma_{xy} = \frac{1}{2\pi(\kappa+1)}[p_x H_{11}(x,y;\xi)+p_y H_{12}(x,y;\xi)], \tag{1f}$$

$$\sigma_{yy} = \frac{1}{2\pi(\kappa+1)}[p_x H_{13}(x,y;\xi)+p_y H_{14}(x,y;\xi)], \tag{1g}$$

where G is the shear modulus. The constant $\kappa = (3-4\nu)$ for plane strain and $\kappa = (3-\nu)/(1+\nu)$ for plane stress, where ν is the Poisson's ratio. The details of the kernels H_1–H_{14} are given in the Appendix; they were obtained from Dundurs and Hetenyi (1961) and Hetenyi and Dundurs (1962) using MATHEMATICA (Wolfram, 1991).

The fundamental solutions at (x,y) for a two-dimensional half plane subjected to an edge dislocation with Burger's vector components b_x and b_y acting at a point $(\xi,0)$ may also be expressed as (Dundurs and Mura, 1964)

$$u_{x,x} = \frac{1}{2\pi(\kappa+1)}[b_x I_1(x,y;\xi)+b_y I_2(x,y;\xi)], \tag{2a}$$

$$u_{x,y} = \frac{1}{2\pi(\kappa+1)}[b_x I_3(x,y;\xi)+b_y I_4(x,y;\xi)], \tag{2b}$$

$$u_{y,x} = \frac{1}{2\pi(\kappa+1)}[b_x I_5(x,y;\xi)+b_y I_6(x,y;\xi)], \tag{2c}$$

$$u_{y,y} = \frac{1}{2\pi(\kappa+1)}[b_x I_7(x,y;\xi)+b_y I_8(x,y;\xi)], \tag{2d}$$

$$\sigma_{xx} = \frac{G}{\pi(\kappa+1)}[b_x I_9(x,y;\xi)+b_y I_{10}(x,y;\xi)], \tag{2e}$$

$$\sigma_{xy} = \frac{G}{\pi(\kappa+1)}[b_x I_{11}(x,y;\xi)+b_y I_{12}(x,y;\xi)], \tag{2f}$$

$$\sigma_{yy} = \frac{G}{\pi(\kappa+1)}[b_x I_{13}(x,y;\xi)+b_y I_{14}(x,y;\xi)]. \tag{2g}$$

The details of the kernels I_1–I_{14} are also given in the Appendix.

It is important to notice here that the displacement gradient fields and the stress fields in eqns (1)–(2) contain a singularity of the order of r as the distance r between the field point (x,y) and the source point $(\xi,0)$ approaches zero. This order of singularity is the same as that for the full plane. The singular behavior for the point load case in a full plane has been discussed widely, particularly in the boundary integral equation literature [e.g. Banerjee and Butterfield (1981), Mukherjee (1982) and Cruse (1988)]. Recently, Dundurs and Markenscoff (1989) also examined the singular behavior for a point dislocation in a full plane. A similar procedure is followed in the present work to represent the singular integrals for the half plane in a Cauchy principal value sense.

4. AN INTEGRAL EQUATION FORMULATION FOR GENERAL CRACK–ANTICRACK SYSTEMS

It is assumed here that the crack, like any other void, cannot transmit any traction. Accordingly, the crack surface is required to be traction free. For the purpose of this work, any crack closure is neglected, and it is assumed that the crack remains open throughout the application of the external load. The anticrack, like any other rigid inclusion, can only admit rigid-body motions. A perfect bonding between the rigid line and the matrix is assumed here.

A general system containing M cracks and N anticracks embedded in arbitrary orientations in an elastic half plane is considered here. We concentrate on the ith defect (crack or anticrack) and consider a local tangential-normal coordinate system with origin at the center of the defect, the normal direction denoted by $s^{(i)}$, and the tangential direction along the ith crack, or anticrack, denoted by $t^{(i)}$. The coordinates of the center of the ith defect are denoted by $(x_c^{(i)}, y_c^{(i)})$ and the angle between x and $t^{(i)}$ is denoted by $\theta^{(i)}$. This is shown schematically in Fig. 1. The occupancy of the ith defect is denoted as $-a^{(i)} < t^{(i)} < a^{(i)}$. The solution of such a system must meet the following requirements: (1) The stress field must satisfy equilibrium. (2) The free surface must be traction free. (3) Crack surfaces must be traction free. (4) Rigid lines, or anticracks, should undergo only rigid-body motions. These rigid-body motions should not cause any material separations (assuming perfect bonding).

Under the above assumptions, the boundary conditions for the cracks require that $(i = 1, 2, \ldots, M)$

$$\sigma_{ss}^{(i)} = \sigma_{ts}^{(i)} = 0 \quad \text{for } -a^{(i)} < t^{(i)} < a^{(i)}. \tag{3}$$

The boundary conditions for the rigid lines may also be expressed as $(j = 1, 2, \ldots, N)$

$$u_t^{(j)} = \alpha^{(j)} - \omega^{(j)} s^{(j)} \quad \text{and} \quad u_s^{(j)} = \beta^{(j)} + \omega^{(j)} t^{(j)} \quad \text{for } -a^{(j)} < t^{(j)} < a^{(j)}, \tag{4}$$

where $\alpha^{(j)}$ and $\beta^{(j)}$ are the rigid-body translations in the $t^{(j)}$ and $s^{(j)}$ directions, respectively, and $\omega^{(j)}$ is the rigid-body rotation in the $t^{(j)}$–$s^{(j)}$ plane.

The rigid-body displacements may be differentiated with respect to $t^{(j)}$, yielding the boundary conditions $(j = 1, 2, \ldots, N)$

$$\frac{\partial u_t^{(j)}}{\partial t^{(j)}} = 0 \quad \text{and} \quad \frac{\partial u_s^{(j)}}{\partial t^{(j)}} = \omega^{(j)} \quad \text{for } -a^{(j)} < t^{(j)} < a^{(j)} \tag{5}$$

for anticracks, or rigid lines.

Let us now consider the effects of all cracks and anticracks on the mth crack. For consistency, the stress fields associated with different cracks and anticracks are transformed to the local tangential-normal $(t^{(m)}, s^{(m)})$ coordinate system for the mth crack. For example,

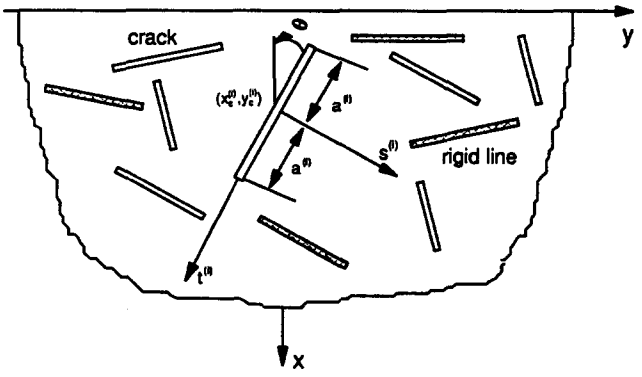

Fig. 1. Schematic diagram of cracks and rigid lines near a free surface.

the stress fields associated with the ith crack may be transformed as

$$\sigma_{ss}^{(m)} = \sigma_{tt}^{(i)} \sin^2 \theta^{(mi)} - 2\sigma_{ts}^{(i)} \sin \theta^{(mi)} \cos \theta^{(mi)} + \sigma_{ss}^{(i)} \cos^2 \theta^{(mi)} \tag{6a}$$

and

$$\sigma_{ts}^{(m)} = (\sigma_{ss}^{(i)} - \sigma_{tt}^{(i)}) \sin \theta^{(mi)} \cos \theta^{(mi)} + \sigma_{ts}^{(i)} (\cos^2 \theta^{(mi)} - \sin^2 \theta^{(mi)}), \tag{6b}$$

where $\theta^{(mi)}$ is the angle between axes $t^{(i)}$ and $t^{(m)}$.

The N anticracks are now represented by their corresponding distribution tractions and the M cracks are represented by their corresponding distributed dislocations. Summing the effects of all cracks and anticracks on the mth crack we get ($m = 1, 2, \ldots, M$)

$$\sum_{i=1}^{M} \int_{-a^{(i)}}^{a^{(i)}} [K_{11}(t^{(m)}, t^{(i)}) b_t^{(i)}(t^{(i)}) + K_{12}(t^{(m)}, t^{(i)}) b_s^{(i)}(t^{(i)})] \, dt^{(i)}$$
$$+ \sum_{j=1}^{N} \int_{-a^{(j)}}^{a^{(j)}} [K_{13}(t^{(m)}, t^{(j)}) p_t^{(j)}(t^{(j)}) + K_{14}(t^{(m)}, t^{(j)}) p_s^{(j)}(t^{(j)})] \, dt^{(j)} + \sigma_{ss}^{(m0)}(t^{(m)}) = 0 \tag{7a}$$

and

$$\sum_{i=1}^{M} \int_{-a^{(i)}}^{a^{(i)}} [K_{21}(t^{(m)}, t^{(i)}) b_t^{(i)}(t^{(i)}) + K_{22}(t^{(m)}, t^{(i)}) b_s^{(i)}(t^{(i)})] \, dt^{(i)}$$
$$+ \sum_{j=1}^{N} \int_{-a^{(j)}}^{a^{(j)}} [K_{23}(t^{(m)}, t^{(j)}) p_t^{(j)}(t^{(j)}) + K_{24}(t^{(m)}, t^{(j)}) p_s^{(j)}(t^{(j)})] \, dt^{(j)} + \sigma_{ts}^{(m0)}(t^{(m)}) = 0, \tag{7b}$$

where $b_t^{(i)}$, $b_s^{(i)}$, $p_t^{(j)}$ and $p_s^{(j)}$ represent the unknown dislocations and tractions on the ith crack and the jth rigid line, respectively; $\sigma_{ss}^{(m0)}$ and $\sigma_{ts}^{(m0)}$ are the stress components at the location of the mth crack but in the absence of all cracks and rigid lines. Here, the kernels K_{11}–K_{24} in eqns (7) may be obtained by transforming the fundamental solution given in the Appendix to an appropriate local coordinate system. The final results may be expressed as

$$K_{11}(t^{(m)}, t^{(i)}) = \frac{G}{\pi(\kappa+1)} \{\cos^2 \theta^{(m)} [\sin \theta^{(i)} I_9(t^{(m)}, t^{(i)}) - \cos \theta^{(i)} I_{10}(t^{(m)}, t^{(i)})]$$
$$+ 2 \sin \theta^{(m)} \cos \theta^{(m)} [\sin \theta^{(i)} I_{11}(t^{(m)}, t^{(i)}) - \cos \theta^{(i)} I_{12}(t^{(m)}, t^{(i)})]$$
$$+ \sin^2 \theta^{(m)} [\sin \theta^{(i)} I_{13}(t^{(m)}, t^{(i)}) - \cos \theta^{(i)} I_{14}(t^{(m)}, t^{(i)})]\}, \tag{8a}$$

$$K_{12}(t^{(m)}, t^{(i)}) = \frac{G}{\pi(\kappa+1)} \{\cos^2 \theta^{(m)} [\cos \theta^{(i)} I_9(t^{(m)}, t^{(i)}) + \sin \theta^{(i)} I_{10}(t^{(m)}, t^{(i)})]$$
$$+ 2 \sin \theta^{(m)} \cos \theta^{(m)} [\cos \theta^{(i)} I_{11}(t^{(m)}, t^{(i)}) + \sin \theta^{(i)} I_{12}(t^{(m)}, t^{(i)})]$$
$$+ \sin^2 \theta^{(m)} [\cos \theta^{(i)} I_{13}(t^{(m)}, t^{(i)}) + \sin \theta^{(i)} I_{14}(t^{(m)}, t^{(i)})]\}, \tag{8b}$$

$$K_{13}(t^{(m)}, t^{(j)}) = \frac{1}{2\pi(\kappa+1)} \{\cos^2 \theta^{(m)} [\sin \theta^{(j)} H_9(t^{(m)}, t^{(j)}) - \cos \theta^{(j)} H_{10}(t^{(m)}, t^{(j)})]$$
$$+ 2 \sin \theta^{(m)} \cos \theta^{(m)} [\sin \theta^{(j)} H_{11}(t^{(m)}, t^{(j)}) - \cos \theta^{(j)} H_{12}(t^{(m)}, t^{(j)})]$$
$$+ \sin^2 \theta^{(m)} [\sin \theta^{(j)} H_{13}(t^{(m)}, t^{(j)}) - \cos \theta^{(j)} H_{14}(t^{(m)}, t^{(j)})]\}, \tag{8c}$$

$$K_{14}(t^{(m)}, t^{(j)}) = \frac{1}{2\pi(\kappa+1)} \{\cos^2 \theta^{(m)} [\cos \theta^{(j)} H_9(t^{(m)}, t^{(j)}) + \sin \theta^{(j)} H_{10}(t^{(m)}, t^{(j)})]$$
$$+ 2 \sin \theta^{(m)} \cos \theta^{(m)} [\cos \theta^{(j)} H_{11}(t^{(m)}, t^{(i)}) - \sin \theta^{(j)} H_{12}(t^{(m)}, t^{(j)})]$$
$$+ \sin^2 \theta^{(m)} [\cos \theta^{(j)} H_{13}(t^{(m)}, t^{(j)}) + \sin \theta^{(j)} H_{14}(t^{(m)}, t^{(j)})]\}, \tag{8d}$$

$$K_{21}(t^{(m)}, t^{(i)}) = \frac{G}{\pi(\kappa+1)}\{\sin\theta^{(m)}\cos\theta^{(m)}[\sin\theta^{(i)}I_9(t^{(m)}, t^{(i)}) - \cos\theta^{(i)}I_{10}(t^{(m)}, t^{(i)})]$$
$$+[\sin^2\theta^{(m)} - \cos^2\theta^{(m)}][\sin\theta^{(i)}I_{11}(t^{(m)}, t^{(i)}) - \cos\theta^{(i)}I_{12}(t^{(m)}, t^{(i)})]$$
$$+\sin\theta^{(m)}\cos\theta^{(m)}[\sin\theta^{(i)}I_{13}(t^{(m)}, t^{(i)}) - \cos\theta^{(i)}I_{14}(t^{(m)}, t^{(i)})]\}, \quad (8e)$$

$$K_{22}(t^{(m)}, t^{(i)}) = \frac{G}{\pi(\kappa+1)}\{\sin\theta^{(m)}\cos\theta^{(m)}[\cos\theta^{(i)}I_9(t^{(m)}, t^{(i)}) + \sin\theta^{(i)}I_{10}(t^{(m)}, t^{(i)}]$$
$$+[\sin^2\theta^{(m)} - \cos^2\theta^{(m)}][\cos\theta^{(i)}I_{11}(t^{(m)}, t^{(i)}) + \sin\theta^{(i)}I_{12}(t^{(m)}, t^{(i)})]$$
$$-\sin\theta^{(m)}\cos\theta^{(m)}[\cos\theta^{(i)}I_{13}(t^{(m)}, t^{(i)}) + \sin\theta^{(i)}I_{14}(t^{(m)}, t^{(i)})]\}, \quad (8f)$$

$$K_{23}(t^{(m)}, t^{(j)}) = \frac{1}{2\pi(\kappa+1)}\{\sin\theta^{(m)}\cos\theta^{(m)}[\sin\theta^{(j)}H_9(t^{(m)}, t^{(j)}) - \cos\theta^{(j)}H_{10}(t^{(m)}, t^{(j)})]$$
$$+[\sin^2\theta^{(m)} - \cos^2\theta^{(m)}][\sin\theta^{(j)}H_{11}(t^{(m)}, t^{(j)}) - \cos\theta^{(j)}H_{12}(t^{(m)}, t^{(j)})]$$
$$-\sin\theta^{(m)}[\sin\theta^{(j)}H_{13}(t^{(m)}, t^{(j)}) - \cos\theta^{(j)}H_{14}(t^{(m)}, t^{(j)})]\}, \quad (8g)$$

$$K_{24}(t^{(m)}, t^{(j)}) = \frac{1}{2\pi(\kappa+1)}\{\sin\theta^{(m)}\cos\theta^{(m)}[\cos\theta^{(j)}H_9(t^{(m)}, t^{(j)}) + \sin\theta^{(j)}H_{10}(t^{(m)}, t^{(j)})]$$
$$+[\sin^2\theta^{(m)} - \cos^2\theta^{(m)}][\cos\theta^{(j)}H_{11}(t^{(m)}, t^{(j)}) + \sin\theta^{(j)}H_{12}(t^{(m)}, t^{(j)})]$$
$$-\sin\theta^{(m)}\cos\theta^{(m)}[\sin\theta^{(j)}H_{13}(t^{(m)}, t^{(j)}) + \sin\theta^{(j)}H_{14}(t^{(m)}, t^{(j)})]\}, \quad (8h)$$

where

$$I(t^{(m)}, t^{(i)}) \equiv I(x, y; \xi) \quad \text{and} \quad H(t^{(m)}, t^{(j)}) \equiv H(x, y; \xi) \quad (9)$$

with x, y and ξ being substituted as ($k = i$ or j)

$$x = x_c^{(m)} + t^{(m)}\cos\theta^{(m)}, \quad (10a)$$
$$y = t^{(k)}\sin\theta^{(k)} - t^{(m)}\sin\theta^{(m)} + y_c^{(m)} - y_c^{(k)}, \quad (10b)$$
$$\xi = x_c^{(k)} + t^{(k)}\cos\theta^{(k)}. \quad (10c)$$

The boundary conditions for anticracks, or rigid lines, are considered next. Utilizing the fact that the components of the displacement gradients transform as

$$u_{t,t}^{(m)} = u_{t,t}^{(j)}\cos^2\theta^{(mj)} + u_{t,s}^{(j)}\sin\theta^{(mj)}\cos\theta^{(mj)} + u_{s,t}^{(j)}\sin\theta^{(mj)}\cos\theta^{(mj)} + u_{s,s}^{(j)}\sin^2\theta^{(mj)} \quad (11a)$$

and

$$u_{s,t}^{(m)} = -u_{t,t}^{(j)}\sin\theta^{(mj)}\cos\theta^{(mj)} - u_{t,s}^{(j)}\sin^2\theta^{(mj)} + u_{s,t}^{(j)}\cos^2\theta^{(mj)} + u_{s,s}^{(j)}\sin\theta^{(mj)}\cos\theta^{(mj)}. \quad (11b)$$

The effects of all cracks and rigid lines on the mth rigid line may be expressed as ($m = 1, 2, \ldots, N$)

$$\sum_{i=1}^{M}\int_{-a^{(i)}}^{a(i)}[K_{31}(t^{(m)}, t^{(i)})b_t^{(i)}(t^{(i)}) + K_{32}(t^{(m)}, t^{(i)})b_s^{(i)}(t^{(i)})]\,dt^{(i)}$$
$$+\sum_{j=1}^{N}\int_{-a^{(j)}}^{(a)^{(j)}}[K_{33}(t^{(m)}, t^{(j)})p_t^{(j)}(t^{(j)}) + K_{34}(t^{(m)}, t^{(j)})p_s^{(j)}(t^{(j)})]\,dt^{(j)} + u_{t,t}^{(m0)}(t^{(m)}) = 0 \quad (12a)$$

and

$$\sum_{i=1}^{M}\int_{-a^{(i)}}^{a(i)}[K_{41}(t^{(m)},t^{(i)})b_t^{(i)}(t^{(i)})+K_{42}(t^{(m)},t^{(i)})b_s^{(i)}(t^{(i)})]\,\mathrm{d}t^{(i)}$$

$$+\sum_{j=1}^{N}\int_{-a^{(j)}}^{(a)^{(j)}}[K_{43}(t^{(m)},t^{(j)})p_t^{(j)}(t^{(j)})+K_{44}(t^{(m)},t^{(j)})p_s^{(j)}(t^{(j)})]\,\mathrm{d}t^{(j)}-\omega^{(m)}(t^{(m)})+u_{s,t}^{(m0)}(t^{(m)})=0 \quad (12b)$$

where $u_{t,t}^{(m0)}$ and $u_{s,t}^{(m0)}$ are the displacement gradients at the location of the mth rigid line, but with no cracks or rigid lines present in the system, and $\omega^{(m)}$ is the rotation of the mth rigid line.

Here, the kernels K_{31}–K_{44} in eqns (12) may also be obtained by transforming the fundamental solution given in the Appendix to an appropriate local coordinate system. The final results may be expressed as

$$K_{31}(t^{(m)},t^{(i)})=\frac{1}{2\pi(\kappa+1)}\{\sin^2\theta^{(m)}[\sin\theta^{(i)}I_1(t^{(m)},t^{(i)})-\cos\theta^{(i)}I_2(t^{(m)},t^{(i)})]$$
$$-\sin\theta^{(m)}\cos\theta^{(m)}[\sin\theta^{(i)}[I_3(t^{(m)},t^{(i)})+I_5(t^{(m)},t^{(i)})]-\cos\theta^{(i)}[I_4(t^{(m)},t^{(i)})+I_6(t^{(m)},t^{(i)})]]$$
$$+\cos^2\theta^{(m)}[\sin\theta^{(i)}I_7(t^{(m)},t^{(i)})-\cos\theta^{(i)}I_8(t^{(m)},t^{(i)})]\}, \quad (13a)$$

$$K_{32}(t^{(m)},t^{(i)})=\frac{1}{2\pi(\kappa+1)}\{\sin^2\theta^{(m)}[\cos\theta^{(i)}I_1(t^{(m)},t^{(i)})+\sin\theta^{(i)}I_2(t^{(m)},t^{(i)})]$$
$$-\sin\theta^{(m)}\cos\theta^{(m)}[\cos\theta^{(i)}[I_3(t^{(m)},t^{(i)})+I_5(t^{(m)},t^{(i)})]+\sin\theta^{(i)}[I_4(t^{(m)},t^{(i)})+I_6(t^{(m)},t^{(i)})]]$$
$$+\cos^2\theta^{(m)}[\cos\theta^{(i)}I_7(t^{(m)},t^{(i)})+\sin\theta^{(i)}I_8(t^{(m)},t^{(i)})]\}, \quad (13b)$$

$$K_{33}(t^{(m)},t^{(j)})=\frac{1}{4\pi G(\kappa+1)}\{\sin^2\theta^{(m)}[\sin\theta^{(j)}H_1(t^{(m)},t^{(j)})-\cos\theta^{(j)}H_2(t^{(m)},t^{(j)})]$$
$$-\sin\theta^{(m)}\cos\theta^{(m)}[\sin\theta^{(j)}[H_3(t^{(m)},t^{(j)})-H_5(t^{(m)},t^{(j)})]-\cos\theta^{(j)}[H_4(t^{(m)},t^{(j)})+H_6(t^{(m)},t^{(j)})]]$$
$$+\cos^2\theta^{(m)}[\sin\theta^{(j)}H_7(t^{(m)},t^{(j)})-\cos\theta^{(j)}H_8(t^{(m)},t^{(j)})]\}, \quad (13c)$$

$$K_{34}(t^{(m)},t^{(j)})=\frac{1}{4\pi G(\kappa+1)}\{\sin^2\theta^{(m)}[\cos\theta^{(j)}H_1(t^{(m)},t^{(j)})+\sin\theta^{(j)}H_2(t^{(m)},t^{(j)})]$$
$$-\sin\theta^{(m)}\cos\theta^{(m)}[\cos\theta^{(j)}[H_3(t^{(m)},t^{(j)})+H_5(t^{(m)},t^{(j)})]+\sin\theta^{(j)}[H_4(t^{(m)},t^{(j)})+H_6(t^{(m)},t^{(j)})]]$$
$$+\cos^2\theta^{(m)}[\cos\theta^{(j)}H_7(t^{(m)},t^{(j)})+\cos\theta^{(j)}H_8(t^{(m)},t^{(j)})]\}, \quad (13d)$$

$$K_{41}(t^{(m)},t^{(i)})=\frac{1}{2\pi(\kappa+1)}\{\sin\theta^{(m)}\cos\theta^{(m)}[\sin\theta^{(i)}[I_1(t^{(m)},t^{(i)})-I_7(t^{(m)},t^{(i)})]$$
$$-\cos\theta^{(i)}[I_2(t^{(m)},t^{(i)})-I_8(t^{(m)},t^{(i)})]]+\sin^2\theta^{(m)}[\sin\theta^{(i)}I_5(t^{(m)},t^{(i)})-\cos\theta^{(i)}I_6(t^{(m)},t^{(i)})]$$
$$-\cos^2\theta^{(m)}[\sin\theta^{(i)}I_3(t^{(m)},t^{(i)})-\cos\theta^{(i)}I_4(t^{(m)},t^{(i)})]\}, \quad (13e)$$

$$K_{42}(t^{(m)},t^{(i)})=\frac{1}{2\pi(\kappa+1)}\{\sin\theta^{(m)}\cos\theta^{(m)}[\cos\theta^{(i)}[I_1(t^{(m)},t^{(i)})-I_7(t^{(m)},t^{(i)})]$$
$$+\sin\theta^{(i)}[I_2(t^{(m)},t^{(i)})-I_8(t^{(m)},t^{(i)})]]+\sin^2\theta^{(m)}[\cos\theta^{(i)}I_5(t^{(m)},t^{(i)})+\sin\theta^{(i)}I_6(t^{(m)},t^{(i)})]$$
$$-\cos^2\theta^{(m)}[\cos\theta^{(i)}I_3(t^{(m)},t^{(i)})+\sin\theta^{(i)}I_4(t^{(m)},t^{(i)})]\}, \quad (13f)$$

$$K_{43}(t^{(m)},t^{(j)})=\frac{1}{4\pi(G\kappa+1)}\{\sin\theta^{(m)}\cos\theta^{(m)}[\sin\theta^{(i)}[H_1(t^{(m)},t^{(j)})-H_7(t^{(m)},t^{(j)})]$$
$$-\cos\theta^{(i)}[H_2(t^{(m)},t^{(j)})-H_8(t^{(m)},t^{(j)})]]+\sin^2\theta^{(m)}[\sin\theta^{(i)}H_5(t^{(m)},t^{(j)})-\cos\theta^{(i)}H_6(t^{(m)},t^{(j)})]$$
$$-\cos^2\theta^{(m)}[\sin\theta^{(i)}H_3(t^{(m)},t^{(j)})-\cos\theta^{(i)}H_4(t^{(m)},t^{(j)})]\}, \quad (13g)$$

$$K_{44}(t^{(m)}, t^{(j)}) = \frac{1}{4\pi(G\kappa+1)}\{\sin\theta^{(m)}\cos\theta^{(m)}[\cos\theta^{(i)}[H_1(t^{(m)}, t^{(j)}) - H_7(t^{(m)}, t^{(j)})]$$
$$+\sin\theta^{(i)}[H_2(t^{(m)}, t^{(j)}) - H_8(t^{(m)}, t^{(j)})]] + \sin^2\theta^{(m)}[\cos\theta^{(i)}H_5(t^{(m)}, t^{(j)}) + \sin\theta^{(i)}H_6(t^{(m)}, t^{(j)})]$$
$$-\cos^2\theta^{(m)}[\cos\theta^{(i)}H_3(t^{(m)}, t^{(j)}) + \sin\theta^{(i)}H_4(t^{(m)}, t^{(j)})]\}, \quad (13h)$$

where

$$I(t^{(m)}, t^{(i)} \equiv I(x, y; \xi) \quad \text{and} \quad H(t^{(m)}, t^{(j)}) \equiv H(x, y; \xi) \quad (14)$$

with x, y and ξ also being transformed as two arguments, $t^{(m)}$ and $t^{(j)}$, according to eqns (10). Here, eqns (7) ensure traction-free conditions on crack surfaces, and eqns (12) ensure compatible rigid-body motions for the rigid lines. The equilibrium conditions and the traction-free conditions at the free surface are automatically satisfied by virtue of the kernels K_{11}–K_{44}.

It can be observed that eqns (7) and (12) give rise to $2(M+N)$ integral equations. In order to solve these equations completely for $b_t^{(i)}$, $b_s^{(i)}$, $p_t^{(j)}$ and $p_s^{(j)}$, however, we need to evaluate $(2M+2N)$ additional constants of integration. It is also important to notice that we need to evaluate the rotations $\omega^{(j)}$ for the N anticracks. This requires N additional equations, bringing the total number of additional equations required to $(2M+3N)$. The $(2M+3N)$ additional equations may be obtained by considering the continuity of the opening shapes of the cracks and the equilibrium conditions for the anticracks. The continuity requirements for crack opening shapes may be expressed as $(i = 1, 2, \ldots, M)$

$$\int_{-a^{(i)}}^{a^{(i)}} b_t^{(i)}(t^{(i)})\,\mathrm{d}t^{(i)} = 0 \quad \text{and} \quad \int_{-a^{(i)}}^{a^{(i)}} b_s^{(i)}(t^{(i)})\,\mathrm{d}t^{(i)} = 0. \quad (15)$$

Assuming that no external force or couple is applied directly on the anticrack, the equilibrium conditions for the anticracks may also be written as $(j = 1, 2, \ldots, N)$

$$\int_{-a^{(j)}}^{a^{(j)}} p_t^{(j)}(t^{(j)})\,\mathrm{d}t^{(j)} = 0, \quad \int_{-a^{(j)}}^{a^{(j)}} p_s^{(j)}(t^{(j)})\,\mathrm{d}t^{(j)} = 0 \quad \text{and} \quad \int_{-a^{(j)}}^{a^{(j)}} t^{(j)} p_s^{(j)}(t^{(j)})\,\mathrm{d}t^{(j)} = 0. \quad (16)$$

Equations (7) and (12), along with the additional constraints of (15) and (16), now provide an integral equation representation of the interactions in a general system involving M cracks and N anticracks at arbitrary orientations. The above representation is based on the fundamental solutions due to a point load and a point dislocation in an elastic half plane.

The integral equations described above can be solved numerically using a Gauss–Chebychev quadrature scheme. The numerical technique proposed by Erdogan *et al.* (1973) for singular integral equations is adapted here and generalized for systems involving cracks and rigid lines near a free surface, with particular attention given to modeling of rotations of rigid lines.

The discretized system contains $2(L-1)(M+N)$ equations (where L is the number of Gauss points on a crack or a rigid line, M is the number of cracks, and N is the number of rigid lines) but $\{2L(M+N)+N\}$ unknowns. The additional $(2M+3N)$ equations are obtained by requiring continuity of crack opening shapes and equilibrium for the rigid lines (Hu and Chandra, 1993b). The interpolation function due to Krenk (1975) is used in the present work to evaluate the SIFs.

The performance of such a polynomial scheme for close spacings of interacting cracks and rigid lines is obviously an important issue in the present context. It is interesting to note that, in their analysis of singular integral equations, Theocaris and Ioakimidis (1977) show that the numerical scheme developed by Erdogan *et al.* (1973) requires only n quadrature points for accurate representations of polynomial functions of order $2n$. As the

spacings between interacting cracks and rigid lines decrease, higher orders of polynomial functions are needed for accurate representations. However, this does not pose any major limitations. For a problem involving equal length collinear cracks with a small tip separation of $0.01a$ (a being the half length of the crack), the present scheme with 30 quadrature points on a crack yielded SIF values within 0.1% of the analytical results of Erdogan (1962). Melin (1983), Li and Hills (1990), and Rubinstein (1990) also adapted a similar scheme to investigate kinked cracks. An alternative scheme using Fourier series expansion was developed by Hori and Nemat-Nasser (1987) for analysing crack interactions at small spacings.

5. NUMERICAL RESULTS

Applications of the proposed integral equation formulation to several example problems involving interactions of cracks and rigid lines near a free surface are presented in this section. The integral equation formulation is based on the fundamental solutions due to a point force and a point dislocation in an elastic half plane and can handle arbitrary orientations and distributions of cracks and rigid lines, along with arbitrary loading conditions, in the context of elasticity. Thus, the proposed formulation is suitable for investigating the effects of microdefects in ceramics and intermetallics under general loading conditions.

In this paper, the numerical results from the proposed integral equation formulation are first verified against existing solutions for special cases in the literature. Problems involving general systems of cracks and rigid lines near a free surface are addressed next, and the implications of these interactions for ceramic grinding processes are discussed.

In the following presentation, the Poisson's ratio (ν) is taken to be 0.25. If not otherwise specified, the reported stress intensity factors (SIFs) are always normalized with respect to those of a single crack in an infinite plane subject to the same loading. The singular intensities of tangential (P_t) and normal (P_s) tractions for rigid lines are also normalized with respect to the tangential traction singularity (P_0) for a rigid line in an infinite plane subject to the same magnitude of remote normal traction (Wang *et al.*, 1985).

A rigid line normal to the free surface and subject to a remote tension is considered in Fig. 2. The results obtained from the present analysis agree very well with those obtained by Atkinson (1973). (Note that the lower and upper tip SIFs reported by Atkinson involve a transformation constant. To eliminate this constant, the ratio of the upper tip SIF to the lower tip SIF is used here.) It should be noted that the intensity of the tangential traction singularity at the lower tip $[P_t(+1)]$ is stronger than that at the upper tip $[P_t(-1)]$. This is contrary to the variations of SIFs for a corresponding crack problem. As expected, the

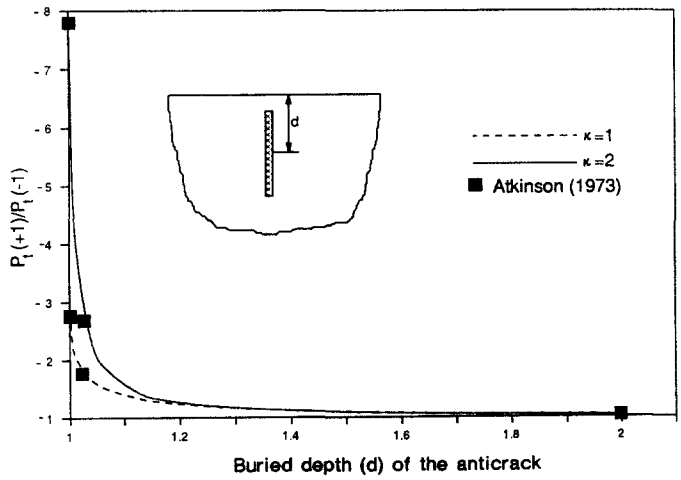

Fig. 2. Variations in $P_t(+1)/P_t(-1)$ with the buried depth of a rigid line (anticrack).

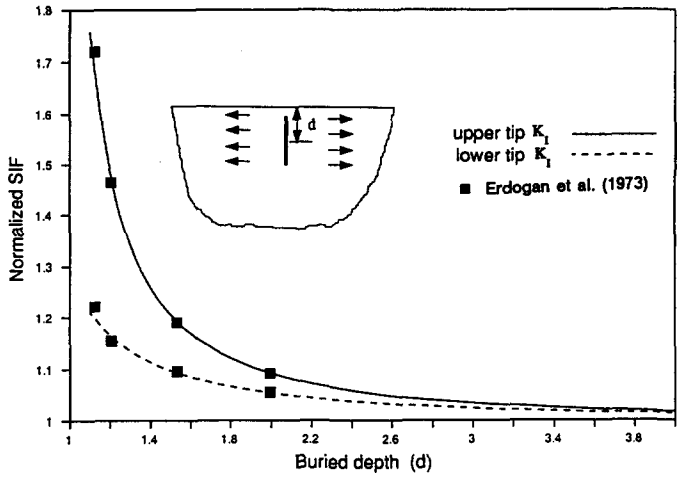

Fig. 3. Variations in normalized SIF with the buried depth of a crack.

intensities at both tips tend to become equal as the buried depth is increased. Figure 3 shows a pressurized crack normal to the free surface. As the buried depth decreases, the free surface amplifies the upper tip SIF considerably. The mode I SIFs obtained from the present analysis also compare very well with those obtained by Erdogan *et al.* (1973). An inclined crack at a normalized buried depth of 1.1 and subject to a remote tension is considered in Fig. 4. The mode I SIFs reach a maximum when the crack is normal to the free surface, while the mode II SIFs attain their absolute maxima of 0.63 for the upper tip and 0.48 for the lower tip at $\theta = 50°$ and $\theta = 43°$, respectively. As shown in Fig. 4, the predictions from the present analysis also agree very well with the results obtained by Nowell and Hills (1987). An inclined rigid line (anticrack) at a normalized buried depth of 1.2 and subject to a remote tension is considered in Fig. 5. Figure 5(a) shows that the absolute maxima for normalized tangential traction intensity (P_t/P_0) occur for both upper and lower tips at $\theta = 0°$. As shown in Fig. 5(b), the free surface makes the normal traction intensities (P_s/P_0) at the upper and lower tips deviate significantly from each other. It is important to observe from Figs 5(a) and 5(b) that, for $\theta = 60°$, the singular intensities vanish for both tangential and normal tractions. Wang *et al.* (1985) show that there exists an orientation, for a rigid line in an infinite plane, for which the traction singularities at the tips of the rigid line disappear. Figures 5(a) and 5(b) establish that similar situations may also occur for a rigid line near a free surface. Figure 5(c) shows the variations in rigid-body

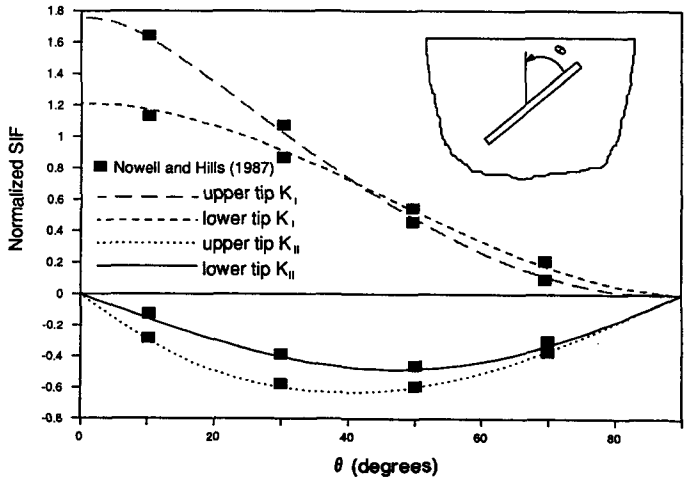

Fig. 4. Variations in normalized SIF with the orientation of a crack.

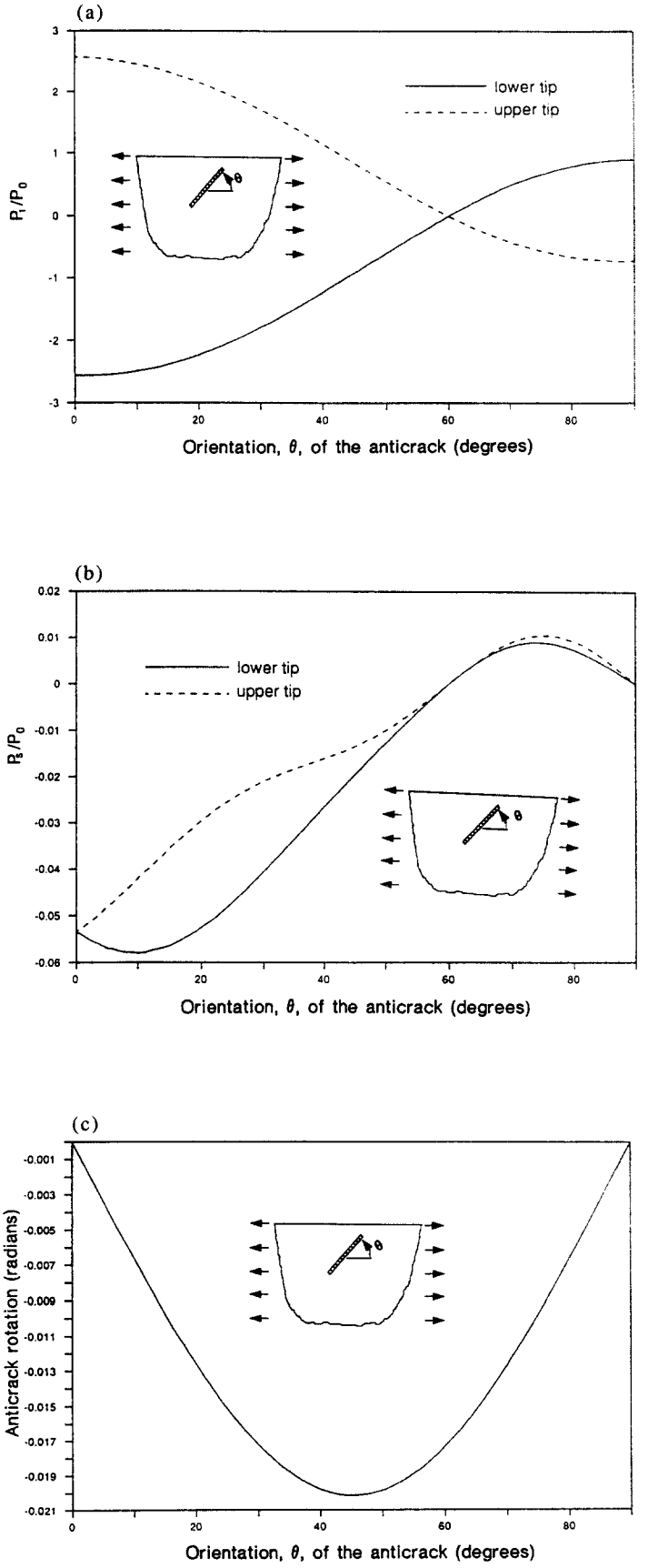

Fig. 5. Orientations of a rigid line (anticrack): (a) With variations in P_t/P_0; (b) With variations in P_s/P_0; (c) With variations in the angular rotation of the line.

rotations with the orientations of the rigid line. The maximum rotation of -0.02 radians (a negative sign implies clockwise rotation) occurs at $\theta = 45°$.

The inset in Fig. 6 shows a crack (normalized buried depth = 0.5) in between two parallel rigid lines (normalized buried depths of 0.4 and 0.6) subject to a remote loading, σ_0. This configuration produces significant mode I and mode II SIFs induced by interactions among the crack and the rigid lines. The mode I SIF (normalized by $\sigma_0\sqrt{\pi a}$) reaches a maximum value of 0.7 at $b = 0.92$; the mode II SIF reaches a value of -0.5 at $b = 1.63$ (a is the half length of the crack, σ_0 the remote tension parallel to the crack, and b the ratio of lengths between the rigid lines and the crack). This is contrary to what is observed for cracks parallel to the direction of loading. In the present case, however, $u_{t,t}$ and $u_{s,t}$ [in eqns (12)] will not necessarily be zero. This will produce nonzero p_s and p_t, which in turn will require nonzero b_s and b_t. Thus, nonzero SIFs may be induced at crack tips.

The interactions between a crack and rigid line with arbitrary relative orientations are considered next. The predictions from the present analysis at large buried depths are first verified against the full plane solution (Hu and Chandra, 1992b). As shown in Fig. 7(a), the results from the present analysis at a buried depth of $100a$ (a is the half length of the crack) matches very well with the full plane solution. For the current example, the normalized distance between the centers of the crack and the rigid line is 1.2 (note that $0 < \theta < 180°$—the crack and the rigid line are never allowed to overlap); the crack and rigid line are of equal length. The normalized SIFs for a normalized buried depth of 1.2 for the crack and rigid-line centers are presented in Fig. 7(b). The normalized mode I SIF at the crack tip near the rigid line reaches a minimum value of 0.55 at $\theta = 100°$. The normalized mode II SIF for the near tip varies noticeably from -0.55 at $\theta = 5°$ to 0.41 at $\theta = 173°$ and passes through zero at $\theta = 104°$. Due to effects of the free surface, the position of the zero value deviates from $\theta = 90°$. The far-tip SIFs are not significantly affected by variations in the orientation of the accompanying rigid line. Figure 7(c) shows the variations of normalized traction singularities for the rigid line with its orientation. Compared to the full plane solutions (Hu and Chandra, 1992b), the symmetry at the lower tip (about $\theta = 90°$) is only slightly modified due to effects of the free surface. However, P_t/P_0 for the upper tip reaches a maximum of 0.44 at $\theta = 120°$, which deviates considerably from the $\theta = 90°$ position of the maximum for the full plane. The variation in the rotations of the rigid line with its orientation is presented in Fig. 7(d). The rotation reaches 0.0039 radians in the counterclockwise direction for $\theta = 32°$. Then it reverses direction and reaches an extreme value of 0.0068 radians in the clockwise direction at $\theta = 160°$.

Figure 8 shows the shielding between a crack and a rigid line perpendicular to each other. The crack is pressurized. The normalized buried depth of the lower tip of the crack

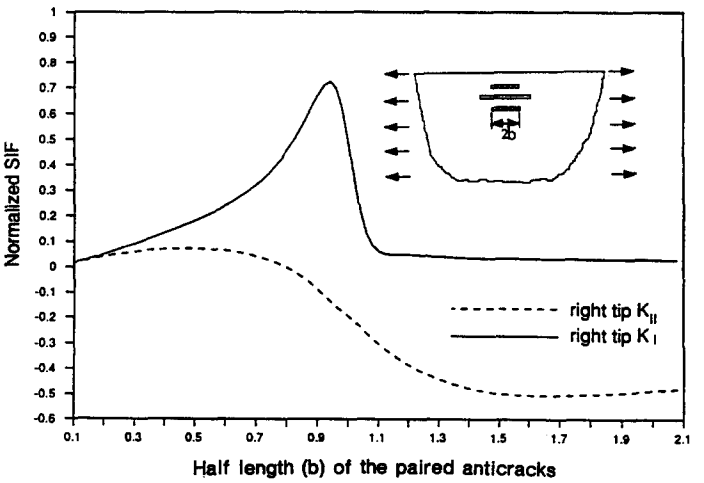

Fig. 6. Coupling-induced stress singularities for a crack in between two parallel rigid lines (anti-cracks).

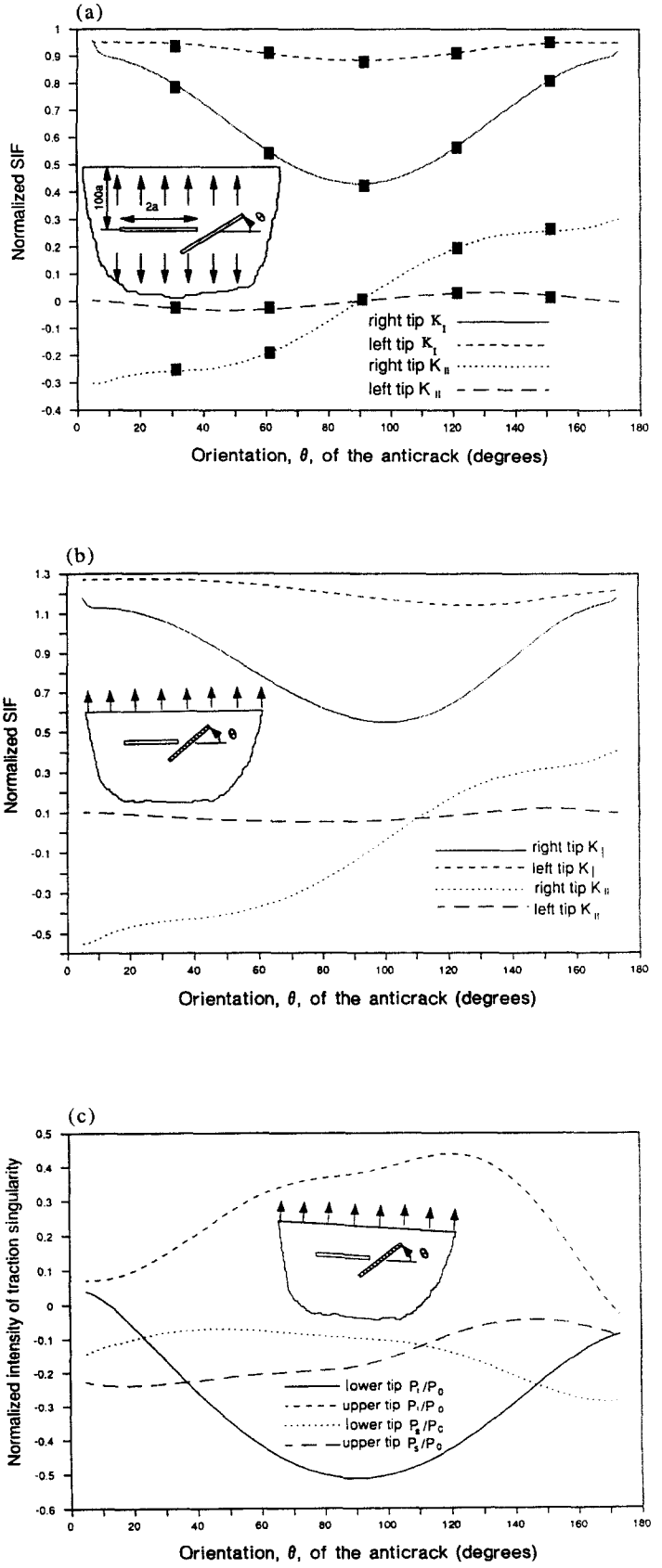

Fig. 7. Interactions between a crack and a rigid line with arbitrary relative orientations: (a) Verification against the full plane solution; (b) Variations in normalized SIF with θ; (c) Variations in P_t/P_0 and P_s/P_0 with θ; (d) Variations in rigid-body rotation of the rigid line with θ.

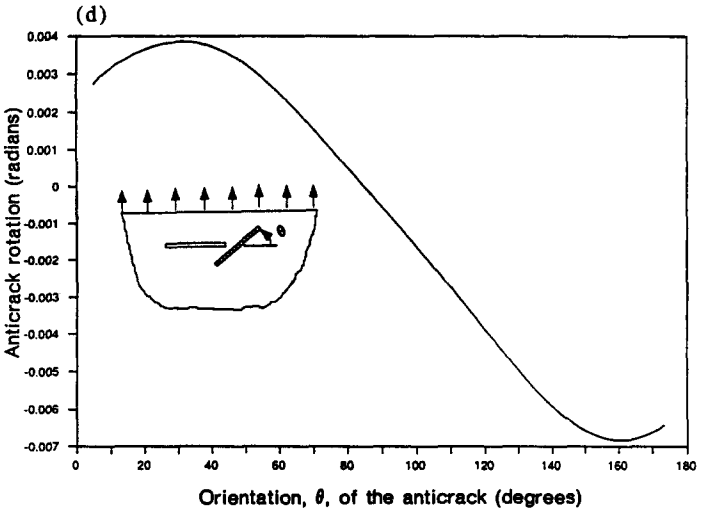

Fig. 7 (*continued*).

is 1.2, and the rigid line is placed at a distance of 0.1 from this crack tip. Such pressurized cracks are typical in indentation problems. The process of grinding ceramics may also be viewed as a moving indentation problem, and such radial cracks are commonly observed in this process. To improve the strength of the finished workpiece, it is important to retard the growth of such cracks normal to the free surface. It is observed, here, that the arrangement shown in Fig. 8 makes the mode I SIF at the lower tip drop from 1.16 to 0.86 as the length of the rigid line is increased from 0.1 to 1.0. The arrangement shown in Fig. 9 has a buried crack depth of 1.2 and a buried depth of 2.2 for the centers of the rigid lines (the lower tip of the crack is aligned with the centers of the rigid lines). The rigid lines are spaced at a distance of 0.1 from each other. The crack is pressurized. As shown in Fig. 9, the mode I SIF at the lower tip rises from 1.16 to 1.28 as the half length of the rigid line is increased to 0.26. This amplification is due to tip interactions that occur in the proximity of the crack and rigid-line tips at short lengths of the rigid line. As the length of the rigid line is increased to 1.0, the mode I SIF at the lower tip drops to 1.18. At the same time, the upper tip mode I SIF is also reduced from 1.46 to 1.28.

6. CONCLUSIONS AND DISCUSSION

The fundamental solutions due to point loads and point dislocations in an elastic half plane are utilized in the present analysis to develop a model for interactions among cracks

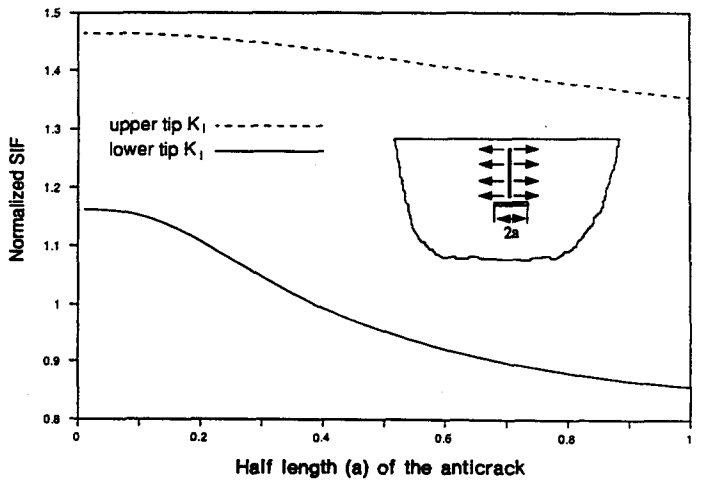

Fig. 8. Shielding effects between a crack and a rigid line perpendicular to each other.

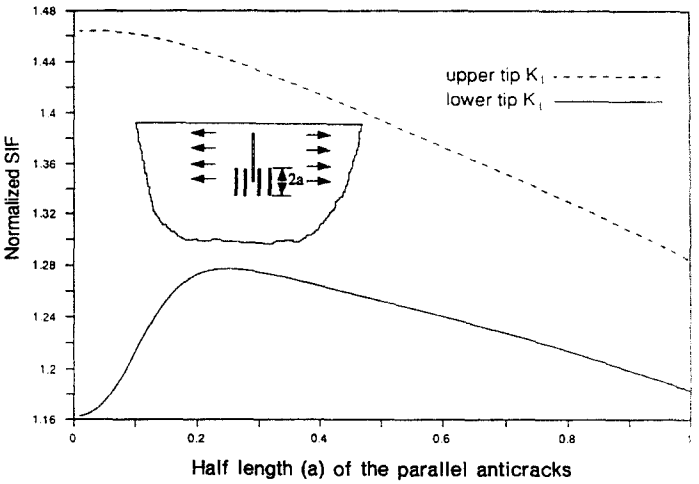

Fig. 9. Interactions between a crack and a system of parallel rigid lines.

and rigid lines (or anticracks) near a free surface in the context of elastic fracture mechanics. An integral equation approach is pursued for this purpose. The proposed technique is capable of handling general loading conditions and arbitrary orientations of cracks and anticracks. A Gauss–Chebychev quadrature is used to reduce the integral equations to a linear system of equations consisting of the distribution of forces and Burger's dislocation vectors, respectively, on the cracks and the anticracks.

The proposed integral equation approach was first verified against existing solutions for a single rigid line (Atkinson, 1973) and single crack (Erdogan *et al.*, 1973; Nowell and Hills, 1987) near a free surface. A system containing two parallel rigid lines separated by a crack near a free surface, subject to a remote loading in the crack direction, was considered next (Fig. 6). It is interesting to observe the existence of nonzero mode II SIFs in such a system. A general crack-rigid line system with arbitrary relative orientations was considered next, and the effects of relative orientations were investigated.

In the grinding of ceramics, one attempts to retard the growth of radial cracks normal to the free surface. This improves the strength of the finished part after grinding. To improve the efficiency of the process and to increase the material removal rate, the designer may also facilitate the growth of lateral cracks parallel to the free surface. Based on our observations of interactions among cracks and rigid lines, a distribution of cracks and rigid lines may be constructed to improve the strength of the finished product, as well as to improve the material removal rate in the grinding of ceramics. Many real-life materials contain hard second-phase whiskers or lamellae that may be modeled as rigid lines. The proposed integral equation approach provides an avenue for investigating general systems of cracks and rigid lines near a free surface. Work on sensitivity studies for such systems and applications to ceramic grinding processes is currently in progress at The University of Arizona.

Acknowledgements—The authors gratefully acknowledge the financial support provided under Grant No. DMC 8657345 from the U.S. National Science Foundation.

REFERENCES

Atkinson, C. (1973). Some ribbon-like inclusion problems. *Int. J. Engng Sci.* **11**, 243–266.

Baeslack, W. A., Cieslak, M. J. and Headley, T. J. (1988). Structure, properties and fracture of pulsed Nd:YAG laser welded Ti-14.8 wt% Al-21.3 wt% Nb titanium aluminide. *Scripta Metall.* **22**, 1155–1160.

Ballarini, R. (1987). An integral equation approach for rigid line inhomogeneity problems. *Int. J. Fract.* **33**, R23–26.

Banerjee, P. K. and Butterfield, R. (1981). *Boundary Element Method in Engineering Science*. McGraw-Hill, London.

Broberg, K. B. (1987). On crack paths. *Engng Fract. Mech.* **28**, 663–679.

Brussat, T. R. and Westmann, R. A. (1975). A Westergaard-type stress function for line inclusion problems. *Int. J. Solids Structures* **11**, 665–677.

Chatterjee, S. N. (1975). The stress field in the neighborhood of a branched crack in an infinite elastic sheet. *Int. J. Solids Structures* **11,** 521–538.
Chen, Y. Z. (1984). Solutions of multiple crack problems of a circular plate or an infinite plate containing a circular hole by using Fredholm integral equation approach. *Int. J. Fract.* **25,** 155–168.
Cheung, Y. K. and Chen, Y. Z. (1987). Solution of branch crack problems in plane elasticity by using a new integral equation approach. *Engng Fract. Mech.* **28,** 31–41.
Chou, Y. T. and Wang, Z. Y. (1983). Stress singularity at the tip of a rigid flat inclusion. In *Recent Developments in Applied Mechanics* (Edited by F. F. Ling and I. G. Tadjbakhsh), pp. 21–30. Rensselaer Press, New York.
Chudnovsky, A., Dolgopolsky, A. and Kachanov, M. (1987a). Elastic interaction of a crack with a microcrack array—I. Formulation of the problem and general form of the solution. *Int. J. Solids Structures* **23,** 1–10.
Chudnovsky, A., Dolgopolsky, A. and Kachanov, M. (1987b). Elastic interaction of a crack with a microcrack array—II. Elastic solution for two crack configurations (piece-wise constant and linear approximations). *Int. J. Solids Structures* **23,** 11–21.
Cotterell, B. and Rice, J. K. (1980). Slightly curved or kinked cracks. *Int. J. Fract.* **16,** 155–169.
Cruse, T. A. (1988). *Boundary Element Analysis in Computational Fracture Mechanics.* Kluwer Academic Publishers, Dordrecht.
Dundurs, J. and Hetenyi, M. (1961). The elastic plane with a circular insert, loaded by a radial force. *ASME J. Appl. Mech.* **28,** 103–111.
Dundurs, J. and Markenscoff, X. (1989). A Green's function formulation of anticracks and their interaction with load-induced singularities. *ASME J. Appl. Mech.* **56,** 550–555.
Dundurs, J. and Mura, T. (1964). Interaction between an edge dislocation and a circular inclusion. *J. Mech. Phys. Solids* **12,** 177–189.
Erdogan, F. (1962). On the stress distribution on plates with collinear cuts under arbitrary loads. *Proceedings 4th U.S. National Congress of Applied Mechanics*, pp. 547–553. ASME, New York.
Erdogan, F. and Gupta, G. D. (1972). Stress near a flat inclusion in bonded dissimilar materials. *Int. J. Solids Structures* **8,** 533–547.
Erdogan, F. and Gupta, G. D. (1975). The crack problem with a crack crossing the boundary. *Int. J. Fract.* **11,** 13–27.
Erdogan, F., Gupta, G. D. and Cook, T. S. (1973). Numerical solution of singular integral equations. In *Methods of Analysis and Solutions of Crack Problems* (Edited by G. C. Sih), pp. 368–425. Noordhoff, Leyden.
Eshelby, J. D. (1957). The determination of the elastic field of an ellipsoidal inclusion, and related problems. *Proc. R. Soc., Lond.* **A241,** 376–396.
Eshelby, J. D. (1959). The elastic field outside an ellipsoidal inclusion. *Proc. R. Soc., Lond.* **A252,** 561–569.
Goldstein, R. V. and Salganik, R. L. (1974). Brittle fracture of solids with arbitrary cracks. *Int. J. Fract.* **10,** 507–523.
Haritos, G. K., Hager, J. W., Amos, A. K., Salkind, M. J. and Wang, A. S. D. (1988). Mesomechanics: The microstructure–mechanics connection. *Int. J. Solids Structures* **24,** 1081–1096.
Hasebe, N., Keer, L. M. and Nemat-Nasser, S. (1984). Stress analysis of a kinked crack initiating from a rigid line inclusion; Part 1: Formulation. *Mech. Mater.* **3,** 131–145.
Hetenyi, M. and Dundurs, J. (1962). The elastic plane with a circular insert, loaded by a tangentially directed force. *ASME J. Appl. Mech.* **29,** 362–368.
Hori, M. and Nemat-Nasser, S. (1987). Interacting micro-cracks near the tip in the process zone of a macro-crack. *J. Mech. Phys. Solids* **35,** 601–629.
Horii, H. and Nemat-Nasser, S. (1986). Brittle failure in compression: Splitting, faulting and brittle–ductile transition. *Phil. Trans. R. Soc., Lond.* **A319,** 337–374.
Hu, K. X. and Chandra, A. (1993a). A fracture mechanics approach to modeling strength degradation in ceramic grinding processes. *ASME J. Engng Ind.* **115,** 73–84.
Hu, K. X. and Chandra, A. (1993b). Interactions among general systems of cracks and anticracks: An integral equation approach. *ASME J. Appl. Mech.* (in press).
Ioakimidis, N. I. and Theocaris, P. S. (1979). A system of curvilinear cracks in an isotropic half-plane. *Int. J. Fract.* **15,** 299–309.
Jha, S. C., Ray, R. and Clemm, P. J. (1988). Microstructure of Ti3 Al + Nb alloys produced via rapid solidification. *Mater. Sci. Engng* **98,** 395–397.
Kachanov, M. (1985). A simple technique of stress analysis in elastic solids with many cracks. *Int. J. Fract.* **28,** R11–R19.
Kachanov, M. (1987). Elastic solids with many cracks: A simple method of analysis. *Int. J. Solids Structures* **23,** 23–43.
Keer, L. M. and Bryant, M. D. (1983). A pitting model for rolling contact fatigue. *ASME J. Lub. Tech.* **105,** 198–205.
Keer, L. M., Bryant, M. D. and Haritos, G. K. (1982). Subsurface and surface cracking due to Hertzian contact. *ASME J. Lub. Tech.* **104,** 347–351.
Krenk, S. (1975). On the use of the interpolation polynomial for solutions of singular integral equations. *Q. Appl. Math.* **32,** 479–484.
Li, Q. and Ting, T. C. T. (1989). Line inclusions in anisotropic elastic solids. *ASME J. Appl. Mech.* **56,** 556–563.
Li, Y. and Hills, D. A. (1990). Stress intensity factor solutions for kinked surface cracks. *Int. J. Strain Anal.* **25,** 21–27.
Lo, K. K. (1978). Analysis of branched cracks. *J. Appl. Mech.* **45,** 797–802.
Melin, S. (1983). Why do cracks avoid each other? *Int. J. Fract.* **23,** 37–45.
Melin, S. (1986). On singular integral equations for kinked cracks. *Int. J. Fract.* **30,** 57–65.
Mukherjee, S. (1982). *Boundary Element Methods in Creep and Fracture.* Elsevier Applied Science Publishers, Barking.
Müller, W. H. (1989). The exact calculation of stress intensity factor in transformation toughened ceramics by means of integral equations. *Int. J. Fract.* **41,** 1–22.
Mura, T. (1987). *Micromechanics of Defects in Solids* (2nd End). Martinus Nijhoff, Boston.

Mura, T. (1988). Inclusion problems. *ASME Appl. Mech. Rev.* **41,** 15–20.
Muskhelishvili, N. I. (1953). *Some Basic Problems of the Mathematical Theory of Elasticity*. Noorhoof, Groningen.
Nowell, D. and Hills, D. A. (1987). Open cracks at or near free edges. *J. Strain Anal.* **22,** 177–185.
Rubinstein, A. A. (1990). Crack-path effect on material toughness. *J. Appl. Mech.* **57,** 97–103.
Selvadurai, A. S. P. (1980). The displacements of a flexible inhomogeneity embedded in a transversely isotropic elastic medium. *Fiber Sci. Technol.* **14,** 251–259.
Sendeckyj, G. P. (1970). Elastic problems in plane elastostatics. *Int. J. Solids Structures* **6,** 1535–1543.
Stroh, A. N. (1958). Dislocations and cracks in anisotropic elasticity. *Phil. Mag.* **3,** 625–646.
Stroh, A. N. (1962). Steady-state problems in anisotropic elasticity. *J. Math. Phys.* **41,** 77–103.
Theocaris, P. S. and Ioakimidis, N. I. (1977). Numerical integration methods for the solution of singular integral equations. *Q. Appl. Math.* **35,** 173–182.
Wang, Z. Y., Zhang, H. T. and Chou, Y. T. (1985). Characteristics of the elastic field of a rigid line inhomogeneity. *ASME J. Appl. Mech.* **52,** 818–822.
Wang, Z. Y., Zhang, H. T. and Chou, Y. T. (1986). Stress singularity at the tip of a rigid line inhomogeneity under antiplane shear loading. *ASME J. Appl. Mech.* **53,** 459–462.
Wolfram, S. (1991). *Mathematics, A System for Doing Mathematics by Computer* (2nd End). Addison-Wesley, Redwood City, CA.
Zang, W. L. and Gudmundson, P. (1989). An integral equation method for piece-wise smooth cracks in an elastic half-plane. *Engng Fract. Mech.* **32,** 889–897.
Zang, W. L. and Gudmundson, P. (1991). Kinked cracks in an anisotropic plane modeled by an integral equation method. *Int. J. Solids Structures* **27,** 1855–1865.

APPENDIX

The fundamental functions in eqns (1) and (2) are given as

$$H_1(x,y;\xi)=2(2-\kappa)\left(\frac{x_1}{r_1^2}+\frac{x_2}{r_2^2}\right)-4\left(\frac{x_1^3}{r_1^4}+\frac{x_2^3}{r_2^4}\right)-4\xi\left(\frac{1}{r_2^2}-\frac{8x_2^2}{r_2^4}+\frac{8x_2^4}{r_2^6}\right)-8\xi^2\left(\frac{3x_2}{r_2^4}-\frac{4x_2^3}{r_2^6}\right),$$

$$H_2(x,y;\xi)=y\left\{\frac{2}{r_1^2}-\frac{4x_1^2}{r_1^4}+\frac{\kappa^2+2\kappa-1}{r_2^2}-\frac{4\kappa x_2^2}{r_2^4}+8\xi\left(-\frac{(2-\kappa)x_2}{r_2^4}+\frac{4x_2^3}{r_2^6}\right)+8\xi^2\left(\frac{1}{r_2^4}-\frac{4x_2^2}{r_2^6}\right)\right\},$$

$$H_3(x,y;\xi)=y\left\{-\frac{2\kappa}{r_1^2}-\frac{4x_1^2}{r_1^4}-\frac{\kappa^2+1}{r_2^2}-\frac{4\kappa x_2^2}{r_2^4}-8\xi\left(\frac{x_2}{r_2^4}-\frac{4x_2^3}{r_2^6}\right)-8\xi^2\left(\frac{1}{r_2^4}-\frac{4x_2^2}{r_2^6}\right)\right\},$$

$$H_4(x,y;\xi)=\frac{2x_1}{r_1^2}-\frac{4x_1y^2}{r_1^4}+\frac{(\kappa^2+2\kappa-1)x_2}{r_2^2}-\frac{4\kappa x_2y^2}{r_2^4}-4\xi\left(\frac{\kappa}{r_2^2}-\frac{2x_2^2}{r_2^4}-\frac{2\kappa y^2}{r_2^4}-\frac{8x_2^2y^2}{r_2^6}\right)+8\xi^2\left(\frac{x_2}{r_2^4}-\frac{4x_2y^2}{r_2^6}\right),$$

$$H_5(x,y;\xi)=y\left\{2\kappa\left(\frac{1}{r_1^2}+\frac{1}{r_2^2}\right)-4\kappa\left(\frac{x_1^2}{r_1^4}+\frac{x_2^2}{r_2^4}\right)+\frac{\kappa^2-1}{r_2^2}+4\xi\left(\frac{2(2+\kappa)x_2}{r_2^4}-\frac{8x_2^3}{r_2^6}\right)-8\xi^2\left(\frac{1}{r_2^4}-\frac{4x_2^2}{r_2^6}\right)\right\},$$

$$H_6(x,y;\xi)=-\frac{4\kappa x_1^3}{r_1^4}+\frac{(3-\kappa^2)x_2}{r_2^2}-\frac{4x_2^3}{r_2^4}-4\xi\left(\frac{1}{r_2^2}-\frac{8x_2^2}{r_2^4}+\frac{8x_2^4}{r_2^6}\right)+8\xi^2\left(-\frac{3x_2}{r_2^4}+\frac{4x_2^3}{r_2^6}\right).$$

$$H_7(x,y;\xi)=\frac{2x_1}{r_1^2}-\frac{4x_1y^2}{r_1^4}+\frac{2\kappa x_2}{r_2^2}-\frac{4\kappa x_2y^2}{r_2^4}-\frac{(\kappa^2-1)x_2}{r_2^2}+4\xi\left(-\frac{\kappa}{r_2^2}+\frac{2\kappa y^2}{r_2^4}+\frac{2x_2^2}{r_2^4}-\frac{8x_2^2y^2}{r_2^6}\right)$$
$$-8\xi^2\left(\frac{x_2}{r_2^4}-\frac{4x_2y^2}{r_2^6}\right),$$

$$H_8(x,y;\xi)=y\left\{-\frac{2\kappa}{r_1^2}-\frac{2\kappa x_1^2}{r_1^4}-\frac{\kappa^2+1}{r_2^2}-\frac{4x_2^2}{r_2^4}-4\xi\left(-\frac{2x_2}{r_2^4}+\frac{8x_2^3}{r_2^6}\right)+8\xi^2\left(-\frac{1}{r_2^4}+\frac{4x_2^2}{r_2^6}\right)\right\},$$

$$H_9(x,y;\xi)=-\frac{(\kappa-1)x_1}{r_1^2}-\frac{2(\kappa+3)x_1^3}{r_1^4}+\frac{(\kappa-1)x_2}{r_2^2}-\frac{2(3\kappa+1)x_2^3}{r_2^4}+2\xi\left(-\frac{\kappa-1}{r_2^2}+\frac{2(\kappa+5)x_2^2}{r_2^4}-\frac{16x_2^4}{r_2^6}\right)$$
$$-8\xi^2\left(\frac{3x_2}{r_2^4}-\frac{4x_2^3}{r_2^6}\right),$$

$$H_{10}(x,y;\xi)=y\left\{\frac{\kappa-1}{r_1^2}-\frac{4x_1^2}{r_1^4}-\frac{\kappa-1}{r_2^2}-\frac{4\kappa x_2^2}{r_2^4}-4\xi\left(-\frac{(\kappa-1)x_2}{r_2^4}-\frac{16x_2^3}{r_2^6}\right)+8\xi^2\left(\frac{2}{r_2^4}-\frac{4x_2^2}{r_2^6}\right)\right\},$$

$$H_{11}(x,y;\xi)=y\left\{-\frac{\kappa-1}{r_1^2}-\frac{4x_1^2}{r_1^4}+\frac{\kappa-1}{r_2^2}-\frac{4\kappa x_2^2}{r_2^4}+4\xi\left(\frac{(3+\kappa)x_2}{r_2^4}-\frac{8x_2^3}{r_2^6}\right)-8\xi^2\left(\frac{1}{r_2^4}-\frac{4x_2^2}{r_2^6}\right)\right\},$$

$$H_{12}(x,y;\xi)=-\frac{(\kappa+3)x_1}{r_1^2}+\frac{4x_1^3}{r_1^4}-\frac{(3\kappa+1)x_2}{r_2^2}+\frac{4\kappa x_2^3}{r_2^4}-2\xi\left(-\frac{\kappa-1}{r_2^2}+\frac{2(\kappa-7)x_2^2}{r_2^4}+\frac{16x_2^4}{r_2^6}\right)$$
$$+8\xi^2\left(-\frac{3x_2}{r_2^4}+\frac{4x_2^3}{r_2^6}\right),$$

$$H_{13}(x,y;\xi)=\frac{(\kappa-5)x_1}{r_1^2}+\frac{4x_1^3}{r_1^4}-\frac{(5\kappa-1)x_2}{r_2^2}+\frac{4\kappa x_2^3}{r_2^4}+2\xi\left(\frac{\kappa+3}{r_2^2}-\frac{2(\kappa+9)x_2^2}{r_2^4}+\frac{16x_2^4}{r_2^6}\right)-8\xi^2\left(-\frac{3x_2}{r_2^4}+\frac{4x_2^3}{r_2^6}\right),$$

$$H_{14}(x,y;\xi)=y\left\{-\frac{\kappa+3}{r_1^2}+\frac{4x_1^2}{r_1^4}-\frac{3\kappa+1}{r_2^2}+\frac{4\kappa x_2^2}{r_2^4}-4\xi\left(\frac{(\kappa-5)x_2}{r_2^4}+\frac{8x_2^3}{r_2^6}\right)+8\xi^2\left(-\frac{1}{r_2^4}+\frac{4x_2^2}{r_2^6}\right)\right\},$$

$$I_1(x,y;\xi)=y\left\{-\frac{\kappa-1}{r_1^2}-\frac{4x_1^2}{r_1^4}+\frac{\kappa-1}{r_2^2}+\frac{4x_2^2}{r_2^4}-4\xi\left(\frac{(\kappa+3)x_2}{r_2^4}-\frac{8x_2^3}{r_2^6}\right)+8\xi^2\left(\frac{2}{r_2^4}-\frac{4x_2^2}{r_2^6}\right)\right\},$$

$$I_2(x,y;\xi)=\frac{(\kappa-5)x_1}{r_1^2}+\frac{4x_1^3}{r_1^4}-\frac{(\kappa-5)x_2}{r_2^2}-\frac{4x_2^3}{r_2^4}-2\xi\left(\frac{\kappa-1}{r_2^2}+\frac{2(\kappa-7)x_2^2}{r_2^4}-\frac{16x_2^4}{r_2^6}\right)+8\xi^2\left(\frac{3x_2}{r_2^4}-\frac{4x_2^3}{r_2^6}\right),$$

$$I_3(x,y;\xi)=\frac{(\kappa+3)x_1}{r_1^2}-\frac{4x_1y^2}{r_1^4}-\frac{2(\kappa+2)x_2}{r_2^2}+\frac{4x_2y^2}{r_2^4}-2\xi\left(-\frac{\kappa+1}{r_2^2}+\frac{4x_2^2}{r_2^4}-\frac{2(\kappa-1)y^2}{r_2^4}-\frac{16x_2^2y^2}{r_2^6}\right)$$
$$+8\xi^2\left(\frac{x_2}{r_2^4}-\frac{4x_2y^2}{r_2^6}\right),$$

$$I_4(x,y;\xi)=y\left\{\frac{\kappa-1}{r_1^2}+\frac{4x_1^2}{r_1^4}-\frac{\kappa-1}{r_2^2}-\frac{4x_2^2}{r_2^4}-4\xi\left(-\frac{(\kappa-1)x_2}{r_2^4}-\frac{8x_2^3}{r_2^6}\right)+8\xi^2\left(\frac{1}{r_2^4}-\frac{4x_2^2}{r_2^6}\right)\right\},$$

$$I_5(x,y;\xi)=-\frac{(\kappa+3)x_1}{r_1^2}+\frac{4x_1^3}{r_2^4}+\frac{(\kappa+3)x_2}{r_2^2}-\frac{4x_2^3}{r_2^4}-2\xi\left(\frac{\kappa+3}{r_2^2}-\frac{2(\kappa+9)x_2^2}{r_2^4}+\frac{14x_2^2}{r_2^6}\right)+8\xi^2\left(-\frac{3x_2}{r_2^4}+\frac{4x_2^3}{r_2^6}\right),$$

$$I_6(x,y;\xi)=y\left\{-\frac{\kappa+3}{r_1^2}+\frac{4x_1^2}{r_1^4}+\frac{\kappa+3}{r_2^2}-\frac{4x_2^2}{r_2^4}-4\xi\left(\frac{(\kappa+3)x_2}{r_2^4}-\frac{8x_2^3}{r_2^6}\right)+8\xi^2\left(\frac{1}{r_2^4}-\frac{4x_2^2}{r_2^6}\right)\right\},$$

$$I_7(x,y;\xi)=y\left\{-\frac{\kappa-1}{r_1^2}+\frac{4x_1^2}{r_1^4}+\frac{\kappa-1}{r_2^2}-\frac{4x_2^2}{r_2^4}+4\xi\left(\frac{(\kappa+3)x_2}{r_2^4}-\frac{8x_2^3}{r_2^6}\right)+8\xi^2\left(-\frac{1}{r_2^4}+\frac{4x_2^2}{r_2^6}\right)\right\},$$

$$I_8(x,y;\xi)=\frac{(\kappa-1)x_1}{r_1^2}+\frac{4x_1y^2}{r_1^4}-\frac{(\kappa-1)x_2}{r_2^2}-\frac{4x_2y^2}{r_2^4}-2\xi\left(-\frac{\kappa-1}{r_2^2}+\frac{4x_2^2}{r_2^4}+\frac{2(\kappa-1)y^2}{r_2^4}-\frac{16x_2^2y^2}{r_2^6}\right)$$
$$+8\xi^2\left(\frac{x_2}{r_2^4}-\frac{4x_2y^2}{r_2^6}\right),$$

$$I_9(x,y;\xi)=y\left\{6\left(-\frac{1}{r_1^2}+\frac{1}{r_2^2}\right)+4y^2\left(\frac{1}{r_1^4}-\frac{1}{r_2^4}\right)-8\xi\left(-\frac{3x_2}{r_2^4}+\frac{4x_2y^2}{r_2^6}\right)-8\xi^2\left(\frac{3}{r_2^4}-\frac{4y^2}{r_2^6}\right)\right\},$$

$$I_{10}(x,y;\xi)=2\left(\frac{x_1}{r_1^2}-\frac{x_2}{r_2^2}\right)-4y^2\left(\frac{x_1}{r_1^4}+\frac{x_2}{r_2^4}\right)+4\xi\left(\frac{1}{r_2^2}+\frac{2x_2^2}{r_2^4}-\frac{2y^2}{r_2^4}-\frac{8x_2^2y^2}{r_2^6}\right)-8\xi^2\left(\frac{x_2}{r_2^4}-\frac{4x_2y^2}{r_2^6}\right),$$

$$I_{11}(x,y;\xi)=2\left(\frac{x_1}{r_1^2}-\frac{x_2}{r_2^2}\right)-4y^2\left(\frac{x_1}{r_1^4}+\frac{x_2}{r_2^4}\right)+4\xi\left(-\frac{1}{r_2^2}+\frac{8x_2^2y^2}{r_2^6}\right)+8\xi^2\left(\frac{x_2}{r_2^4}-\frac{4x_2y^2}{r_2^6}\right),$$

$$I_{12}(x,y;\xi)=y\left\{2\left(-\frac{1}{r_1^2}+\frac{1}{r_2^2}\right)+4\left(\frac{x_1^2}{r_1^4}-\frac{x_2^2}{r_2^4}\right)-8\xi\left(\frac{x_2}{r_2^4}-\frac{4x_2^3}{r_2^6}\right)-8\xi^2\left(-\frac{1}{r_2^4}+\frac{4x_2^2}{r_2^6}\right)\right\},$$

$$I_{13}(x,y;\xi)=y\left\{2\left(-\frac{1}{r_1^2}+\frac{1}{r_2^2}\right)+4\left(\frac{x_1^2}{r_1^4}-\frac{x_2^2}{r_2^4}\right)-8\xi\left(-\frac{3x_2}{r_2^4}+\frac{4x_2^3}{r_2^6}\right)-8\xi^2\left(\frac{1}{r_2^4}-\frac{4x_2^2}{r_2^6}\right)\right\},$$

$$I_{14}(x,y;\xi)=6\left(\frac{x_1}{r_1^2}-\frac{x_2}{r_2^2}\right)+4\left(-\frac{x_1^3}{r_1^4}+\frac{x_2^3}{r_2^4}\right)+4\xi\left(-\frac{1}{r_2^2}+\frac{8x_2^2}{r_2^4}-\frac{8x_2^4}{r_2^6}\right)+8\xi^2\left(-\frac{3x_2}{r_2^4}+\frac{4x_2^3}{r_2^6}\right),$$

where

$$r_1^2=x_1^2+y^2 \quad \text{and} \quad r_2^2=x_2^2+y^2,$$
$$x_1=x-\xi \quad \text{and} \quad x_2=x+\xi.$$